Harvesting hydrogen gas from air pollutants with an un-biased gas phase photo-electrochemical cell

Harvesting hydrogen gas from air pollutants with an un-biased gas phase photo-electrochemical cell

Sammy W. Verbruggen,*[a],[b] Myrthe Van Hal,[a] Tom Bosserez,[b] Jan Rongé,[b] Birger Hauchecorne,[a] Johan A. Martens,[b] Silvia Lenaerts[a]

Abstract: The concept of an all-gas-phase photo-electrochemical cell (PEC) producing hydrogen gas from volatile organic contaminated gas and light is presented. Without applying any external bias, organic contaminants are degraded and hydrogen gas is produced in separate electrode compartments. The system works most efficiently with organic pollutants in inert carrier gas. In the presence of oxygen gas, the cell performs less efficiently but still significant photocurrents are generated, showing the cell can be run on organic contaminated air. The purpose of this study is to demonstrate new application opportunities of PEC technology and to encourage further advancement toward photo-electrochemical remediation of air pollution with the attractive feature of simultaneous energy recovery and pollution abatement.

Introduction

Today's society is faced with two persistent demands: sustainable energy production and a healthy living environment. In both contexts, the use of semiconductors for photocatalysis has been identified as an important technology. Heterogeneous photocatalysis has proven to be successful in both light-driven hydrogen production through water splitting,[1,2] as well as for the degradation of organic pollutants in gaseous media.[3] In this study both applications are coupled in a single device; a solid and stand-alone photo-electrochemical (PEC) cell. In doing so part of the energy stored in airborne organic pollutants is recovered by hydrogen production, while mineralizing the contaminants to less harmful CO_2. Oxidation of volatile organic compounds (VOC) occurs at the photo-anode, while hydrogen is produced at the (dark) cathode on the opposite side of a proton-conducting solid electrolyte membrane. It is worth mentioning that also aqueous waste streams can be treated using PEC cells.[4]

This concept of an all-solid PEC cell with oxidation reactions and H_2 evolution in separated compartments was first proposed by Seger and Kamat in 2009.[5] Based on this design we have recently successfully explored the possibility of using water vapor (ambient humid air), rather than liquid water as the anode feed.[6] In the quest for coupling air treatment with energy production in a PEC cell, available literature is scarce. Georgieva et al. showcased the photo-oxidation of organic vapors using a different photo-electrochemical cell by applying additional external bias.[7–9] In addition, the actual H_2 yield was not determined. Meanwhile in our work the absence of external bias is a crucial operating parameter for evolving towards autonomous real-life applications. Although autonomous water splitting using TiO_2 is often regarded difficult due to the overpotential involved in the reaction, it has clearly been shown to be feasible.[5,10] In other reports the gas feed is generated by bubbling an inert carrier gas (e.g. Ar) through a gas wash bottle containing a solution of organic contaminants.[11] When considering air pollution, however, the presence of oxygen in the gas mixture should not be neglected, as it could scavenge the photogenerated electrons at the photo-anode, rendering them unavailable for H_2 evolution.[12] In this work we therefore investigate the effect of oxygen on the photocurrent delivered by the cell, but also its effect on the photocatalytic reaction pathway at the photo-anode by on-line FTIR analysis of the anode gas outlet. This should lead to a better understanding and fast development of stand-alone (*i.e.* un-biased) gas-phase photo-electrochemical devices for converting air pollution to energy.

Results and Discussion

Aqueous phase experiments

As a first short test the cell's capacity for organic waste water remediation was studied. Methanol was selected as a model compound, as it is convenient to study and it is the best available system described in literature. Different aqueous methanol solutions were prepared with concentrations of 0, 0.1, 1 and 5 wt%. In first instance the solutions were purged with N_2 gas to remove all oxygen. Next, the purged solutions were pumped through the serpentine flow channels of the anode compartment at a pumping speed of 1.2 mL min^{-1}. After 1 h equilibration in dark conditions, a chrono-amperometric measurement was started under UV illumination. The I-t plots for all four solutions are given in Figure 1a. It can be derived that a methanol concentration of 0.1 wt% hardly influences the generated photocurrent and basically remains at the same level as pure water (around 10 µA cm^{-2}). At higher methanol content the photocurrent density increases to a level of ca. 25 µA cm^{-2} for 1 wt% (an increase of a factor of 2.5 compared to pure H_2O) and 45 µA cm^{-2} for 5 wt% (an increase of a factor 4.5 compared to pure water). The observed increase in photocurrent is comparable to the findings of Seger and Kamat, who observed a 3-fold increase in photocurrent for a 1 wt% MeOH solution compared to pure water.[5] In absolute number, however, the photocurrent obtained in their work is almost one order of magnitude higher, which is evident due to a larger photocatalyst loading at the anode, the presence of 0.1 M H_2SO_4 as an electrolyte and a much stronger irradiation source.

[a] Prof. dr. S.W. Verbruggen,* ir. M. Van Hal, Dr. B. Hauchecorne, Prof. dr. S. Lenaerts
Department of Bioscience Engineering
University of Antwerp
Groenenborgerlaan 171, 2020 Antwerp, Belgium
*E-mail: Sammy.verbruggen@uantwerp.be
[b] Prof. dr. S.W. Verbruggen,* ir. T. Bosserez, Dr. J. Rongé, Prof. dr. J.A. Martens
Department of Microbial and Molecular Systems
KU Leuven
Celestijnenlaan 200F, 3001 Heverlee, Beglum

Next, the influence of oxygen on the generated photocurrent is investigated. For this experiment all solutions were purged with synthetic air for 1 h, prior to each chrono-amperometric measurement. The results are presented in Figure 1b. Fortunately, the trend of increasing photocurrent density with increasing methanol content is well retained. On the other hand an average decrease of 40% is observed compared to the photocurrent density generated under N_2-purge. This effect is explained by electron scavenging of O_2 molecules at the photo-anode with the formation of superoxide anions ($O_2^{-\bullet}$),[12] alike the observed recombination process of photogenerated electrons with I_3^- ions at the semiconductor-electrolyte interface in dye sensitized solar cells.[13] Nonetheless, the available photocurrent is still almost 3 times higher in the presence of organic pollution compared to pure photo-electrochemical water splitting.

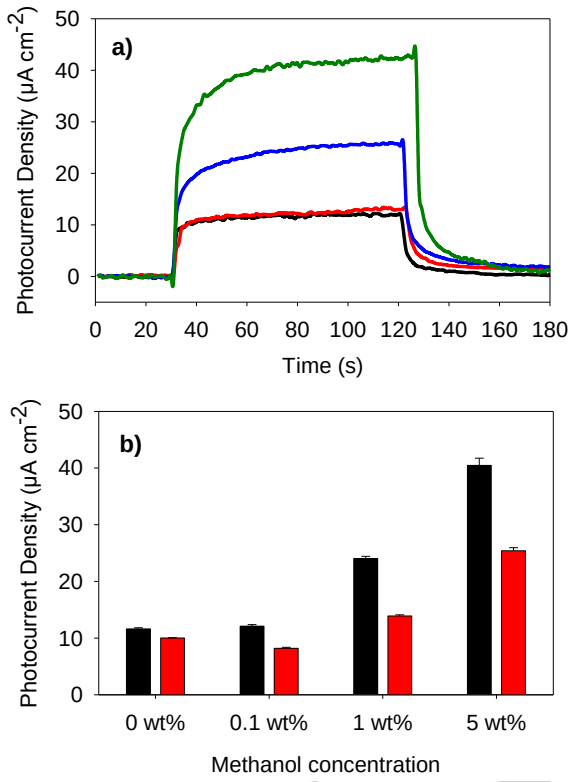

Figure 1. a) Chrono-amperometric (I-t) plots obtained for N_2-purged aqueous solutions of methanol at concentrations of 0 wt% (black), 0.1 wt% (red), 1 wt% (blue) and 5 wt% (green) as the photo-anode feed. b) Photocurrent density obtained for different aqueous methanol solution in the absence (black bars) and in the presence (red bars) of dissolved oxygen. All experiments are carried out without applying any external bias.

Gas phase experiments

After benchmarking the cell in aqueous phase and evaluating the effect of dissolved oxygen, the PEC cell was tested for gas treatment. A gas wash bottle was filled with pure water or the 5 wt% MeOH solution and mounted in a fully automated gas analysis setup.[14] A steady flow of N_2 gas was bubbled through the bottle at a constant rate of 50 mL min^{-1}. A humidity sensor (Vaisala) was connected to the gas outlet and 65% relative humidity was measured. For studying the photo-electrochemical air treatment performance in realistic conditions, i.e. in the presence of 21% O_2, the carrier gas was changed from N_2 to compressed air (Messer). The chrono-amperometric measurements under UV illumination were performed over a time span of 20 min to enable the detection of all formed intermediates and mineralization products by infrared spectroscopy of the gas outlet (see below). The resulting I-t plots in the presence and absence of methanol vapor, when using an inert or an oxygenated carrier gas, are shown in Figure 2a.

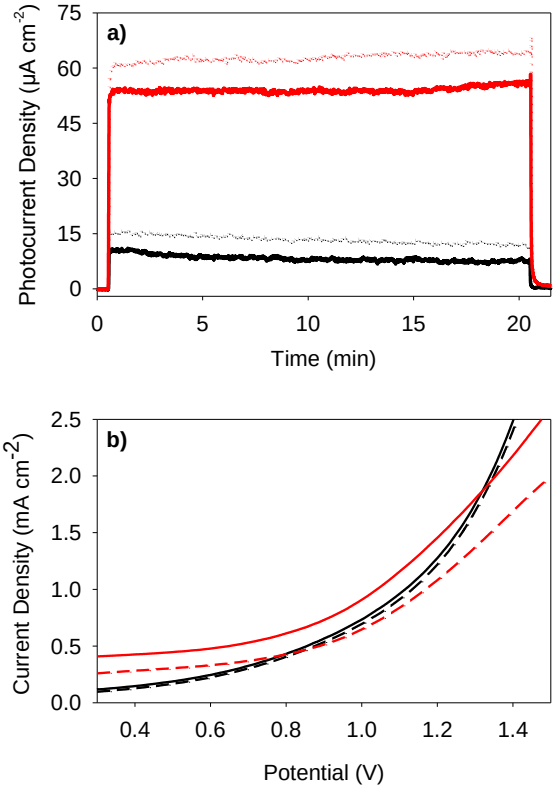

Figure 2. a) Chrono-amperometric (I-t) plots obtained for pure water vapor (black) and water-methanol vapor (red) using air (solid lines) or N_2 (dotted lines) as the carrier gas. No external bias was applied. UV on at t = 1 min, UV off at t = 21 min. b) J-V sweeps (50 mV s^{-1}) obtained for pure water vapor (black) and water methanol vapor (red) in air, both in dark (dashed lines) and under UV illumination (solid lines).

The first striking observation is that under inert atmosphere, the photocurrent densities for water vapor as well as methanol vapor are about 30% higher compared to their liquid-phase equivalents (*cfr.* Figure 1). This could be due to the absence of diffusion limitations in the gas phase.[15] Secondly, the increase in photocurrent in the presence of methanol vapor compared to pure water vapor is again a factor of 4.5, thus similar to the aqueous phase measurements. Finally and more importantly, the effect of oxygen is not as detrimental in gas phase as in aqueous phase. For the methanol-rich vapor feed, a current

decrease of only 8% is observed in air instead of inert N_2 as the carrier gas, resulting in a photocurrent that is ca. 5 times higher compared to pure water vapor.

J-V cell characteristics using air as the carrier gas are presented in Figure 2b. First of all it is evident that under UV illumination higher current densities are achieved then in dark conditions. This effect is much more pronounced in the presence of methanol, which is in line with previous experiments. As soon as the potential for water electrolysis is exceeded, higher photocurrent density can be drawn from water vapor rather than from methanol vapor. At least in part, this could be due to competition between water electrolysis and photo-electrochemical methanol degradation in favor of the former process when operating the cell at higher potentials. In view of the application of pollutant abatement, this is again a good motivation to operate the cell at low, preferentially even no electrical bias, as is the scope of this investigation.

It is clear this is a very encouraging result that spurs further investigation of PEC-based air treatment for energy recovery. In addition, it should be stressed again that all these results are obtained without applying external bias and the electrode materials are not yet fully optimized towards cell performance.[16] This proof of concept is thus an important step in the development of stand-alone PEC cells for simultaneous pollutant abatement and energy recuperation, but still offers ample room for improvement in follow-up studies. For instance, ongoing investigations by our group involve modification of the anode material with plasmonic alloy nanoparticles, of which we have shown they can span the entire UV-VIS spectrum hereby effectively increasing solar photon utilization.[17,18]

As mentioned above, all gaseous species formed during photo-oxidation at the anode are analyzed by infrared spectroscopy. In order to facilitate the analysis, a representative spectrum of the steady-state gas outlet in dark condition is subtracted from a representative spectrum obtained during illumination (more precisely, after 18 min continuous illumination). These FTIR difference spectra are plotted in Figure 3 for both the situations in which N_2 (blue) or air (red) is used as the carrier gas. The negative bands in the region 2700 - 3100 cm^{-1} corresponding to the C-H stretching vibrations of methanol confirm its disappearance. The mineralization of methanol is furthermore evidenced by the formation of CO_2 (2290-2390 cm^{-1}), that is not attributed to the decomposition of Toray paper, as verified by blanc experiments. Comparison of the integrals of the CO_2 bands in this wavenumber region for both carrier gases, reveals 20% more complete mineralization when air is used. In that case O_2 is involved directly in the photo-oxidation process through, for instance, $O_2^{-\bullet}$ radical-initiated pathways after scavenging of photogenerated electrons by O_2 molecules. This is also in line with the observed decrease in photocurrent in the presence of O_2, which clearly exposes a tradeoff between more complete pollutant abatement (mineralization to CO_2) *versus* photocurrent generation and consecutive H_2 production.

The FTIR difference spectra also reveal additional features that are not ascribed to methanol. Prominent bands in the regions 870-955 cm^{-1} and 1245-1075 cm^{-1} are observed for both carrier gases. In the presence of oxygen, additional shoulders are observed in the regions 1195-1210 cm^{-1} and 1080-1130 cm^{-1}, that can be related to C-H bending (rocking) vibrations. Typical C-H stretching vibration bands between 2780 and 2960 cm^{-1} are also observed only when oxygen is present. Considering the possible oxidation pathways for methanol in both anaerobic and aerobic conditions, and comparative analysis of the FTIR difference spectra with spectra of possible gaseous intermediates obtained from the NIST database, two stable gaseous intermediate species are identified: methyl formate (MF) and dimethylether (DME) (Figure 3). MF is formed in both anaerobic and aerobic conditions and is thus encountered in both difference spectra. DME is only formed in the presence of oxygen and is responsible for the striking dissimilarities in the FTIR difference spectrum for PEC methanol oxidation in air compared to N_2 carrier gas. Unfortunately the most characteristic infrared bands corresponding to C-O vibrations in the broad region 1250-2100 cm^{-1} cannot be used for fingerprint analysis since the difference spectra are dominated by H_2O-related vibrations in this wavenumber range due to the high humidity level in the experiments.

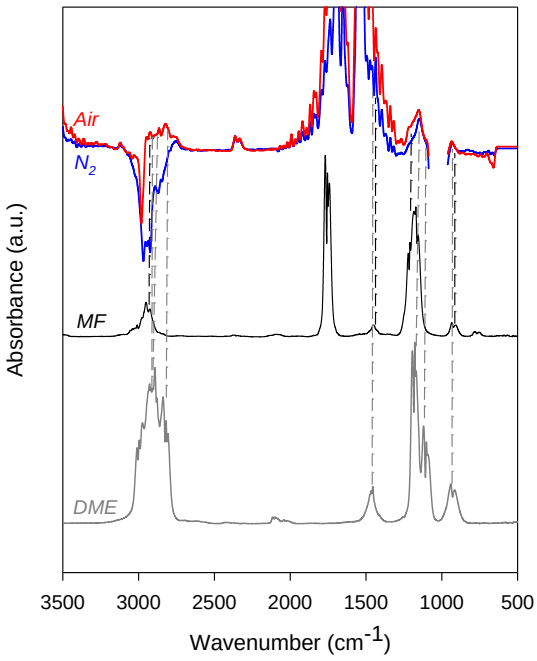

Figure 3. FTIR difference spectra of the anode compartment gas outlet obtained by subtracting the spectrum in dark conditions from the one during illumination, for a methanol-rich vapor feed and using air (red) or inert N2 (blue) as carrier gas. Reference FTIR absorbance spectra of the formed intermediates methyl formate (MF, black) and dimethyl ether (DME, gray) as obtained from the NIST database are also shown and the corresponding absorption bands are indicated by dotted lines. Spectra are smoothed for clarity purposes.

Based on the information above, different reaction pathways can be proposed for the photo-electrochemical treatment of methanol in either the absence or presence of oxygen. The

formation of MF in anaerobic conditions is assumed to proceed through the formation of methoxy radical species after oxidation by •OH radicals (Eq. 1).[19] Consecutive oxidation by •OH radicals will eventually result in the formation of formic acid (Eq. 2-4)[19] and yields MF after reaction with methanol (Eq. 5).

$CH_3OH + •OH\ (or\ h^+) \rightarrow CH_3O• + H_2O\ (or\ H^+)$ (Eq. 1)
$CH_3O• + •OH\ (or\ h^+) \rightarrow H_2CO + H_2O\ (or\ H^+)$ (Eq. 2)
$H_2CO + •OH\ (or\ h^+) \rightarrow HCO^• + H_2O\ (or\ H+)$ (Eq. 3)
$HCO• + •OH \rightarrow HCOOH$ (Eq. 4)
$HCOOH + CH_3OH \rightarrow HCOOCH_3 + H_2O$ (Eq. 5)

Summarizing, the overall anaerobic photo-oxidation of methanol to methyl formate is given by (Eq. 6):

$2\ CH_3OH + 4\ •OH \rightarrow HCOOCH_3 + 4\ H_2O$ (Eq. 6)

In the presence of O_2, MF formation from methanol can be also be achieved by participation of superoxide anions, after reduction of O_2 by photogenerated electrons with the formation of bidendate-formate bound to the catalyst surface (Eq. 7-9).[20] Ultimately MF is formed by radical attack of a methoxy species (Eq. 10).

$2\ CH_3OH + 2\ •OH \rightarrow 2\ CH_3O• + 2\ H_2O$ (Eq. 7)
$e^- + O_2 \rightarrow O_2^{-•}$ (Eq. 8)
$CH_3O• + O_2^{-•} \rightarrow HCOO_{(ads)} + H_2O + e^-$ (Eq. 9)
$HCOO_{(ads)} + CH_3O• \rightarrow HCOOCH_3 + ½\ O_{2(ads)}$ (Eq. 10)

Overall, MF formation through aerobic photo-oxidation of methanol is given by (Eq. 11):

$2\ CH_3OH + 2\ •OH + ½\ O_2 \rightarrow HCOOCH_3 + 3\ H_2O$ (Eq. 11)

Next, we suggest a plausible mechanism for the formation of DME from methanol under UV illumination that can be described as light-induced acid-type catalyzed methanol dehydration, facilitated by $O_2^{-•}$. As in regular acid-like methanol dehydration to DME,[21] the reaction proceeds in three main steps: (i) protonation, (ii) nucleophilic substitution (with dehydration) and (iii) deprotonation. It is known that UV illumination of a TiO_2 surface induces superhydrophilic properties,[22–24] and entails an increased amount of surface hydroxyl groups that render the surface more acidic. This way it can assist in the initial protonation of methanol (Eq. 12). Next step is a nucleophilic attack by a second methanol molecule (Eq. 13). Finally, deprotonation of the formed intermediate is assumed to be largely facilitated by superoxide radicals as strong nucleophiles, with the formation of •OOH (Eq. 14). The latter can further react to •OH or H_2O for surface re-hydroxylation.

$CH_3OH + H^+ \rightarrow 2\ CH_3OH_2^+$ (Eq. 12)
$CH_3OH_2^+ + CH_3OH \rightarrow CH_3\text{-}OH^+\text{-}CH_3 + H_2O$ (Eq. 13)
$e^- + O_2 \rightarrow O_2^{-•}$ (Eq. 8)
$CH_3\text{-}OH^+\text{-}CH_3 + O_2^{-•} \rightarrow CH_3\text{-}O\text{-}CH_3 + •OOH$ (Eq. 14)

Summarizing, the reaction pathway for the aerobic photo-dehydration of methanol to DME can be split into two overall reactions: (i) two molecules of methanol that yield DME and water (Eq. 15), and (ii) photocatalytic oxygen radical formation (Eq. 16).

$2\ CH_3OH \rightarrow CH_3\text{-}O\text{-}CH_3 + H_2O$ (Eq. 15)
$O_2 + e^- + H^+ \rightarrow •OOH$ (Eq. 16)

Finally, a very important conclusion can be drawn from this mechanistic analysis. Note that from (Eq. 16) it is clear that in the aerobic pathway both photogenerated electrons, and H^+ ions are consumed. This will consequently lower the available photocurrent, which corresponds to what we observe experimentally (Figure 2). The same applies to the aerobic photo-oxidation to MF due to participation of $O_2^{-•}$ that is formed by scavenging photogenerated electrons by O_2. This observation highlights an important trade-off when working with PEC cells for (realistic) air treatment: the presence of oxygen will improve the mineralization efficiency of pollutants to CO_2 at the photocatalytic anode, but at the same time opens gateways for the formation of (stable) intermediate species resulting in a lower photocurrent and thus potential hydrogen yield.

H_2 evolution efficiency and future prospect

In the final part of this study the cell's H_2 production efficiency (Faradaic efficiency) is determined. Over a 30 min illumination period 0.41 C of photogenerated charge was produced when feeding the photo-anode with methanol vapor, without applying external bias. This corresponds to a theoretical amount of 0.047 mL H_2 that can potentially be generated. The actual measured amount of H_2 evolution over this 30 min illumination period was 0.044 mL. This results in a Faradaic efficiency of 92%. At this point, it cannot be quantified which fraction of H_2 is originating from methanol or water vapor. Future experiments involving isotope-labeled methanol should enable such relative quantization, but this is outside the scope of the proof-of-concept. For pure water vapor the Faradaic efficiency has been determined to be close to 100%.[6] Under the present conditions an overall energy conversion efficiency of ca. 0.3% can be estimated based on the lower heating value (LHV) of hydrogen gas (120 MJ kg^{-1}) and the total photon flux incident on the cell. While this value obviously appears quite low, it should be reasoned that (when sunlight would be used) this is still a clear net gain in energy resulting from partial abatement of gaseous pollutants, since no bias is applied. Moreover, it was mentioned before that no cell performance optimization has occurred thus far. For instance, the photo-anode material currently relies on un-modified TiO_2, that can only interact with the limited number of UV-photons emitted from the broadband source used in this experiment, hence resulting in a serious under-estimation of the cell's intrinsic efficiency. Altogether these results are thus quite encouraging and indicate that even with a rather simple MEA and cell design, non-negligible hydrogen evolution can be obtained at high Faradaic efficiency. The main challenge for the further exploitation of PEC cells for

air treatment is scaling up towards hydrogen evolution rates of industrial relevance.

As concluding experiments, the versatility of this application has been studied by feeding the anode with air polluted with ethanol and acetic acid, following a similar approach as for methanol. Photocurrent increases of 3.1 and 1.5 were measured with regard to pure water vapor, for ethanol and acetic acid vapors generated from purging aqueous solutions containing 5 wt% of these components, respectively. The order of photocurrent generation for organically contaminated vapor decreases according to methanol > ethanol > acetic acid, for which there are two main explanations. Firstly, the trend follows Henry's law; i.e. starting from 5 wt% solutions, more methanol will be present in the gas phase compared to ethanol or acetic acid and thus a higher partial pressure is achieved. Secondly, the order of photocurrent generation is inversely related to the photo-electrochemical VOC oxidation redox potential of these components: CH_3OH/CO_2 (+0.03 V) < C_2H_5OH/CO_2 (+0.08 V) < CH_3COOH/CO_2 (+0.12 V). These results again illustrate the potential of this technology for environmental remediation with simultaneous energy recovery (as current or H_2) with only light as energy input. We are hopeful this study will bring about the further development of stand-alone gas phase PEC devices towards industrial applications.

Conclusions

In this work the use of a photo-electrochemical (PEC) cell for simultaneous pollutant abatement and energy recovery was investigated. An important operating condition is that no external bias was applied in any of the experiments and only light (representative for solar radiation) is used as additional energy input. Using methanol as a model pollutant, the influence of oxygen on the PEC cell performance was investigated for both aqueous solutions and, more importantly, contaminated gas flows. It was confirmed that increasing the concentration of methanol also increases the generated photocurrent, up to the point where an aqueous 5 wt% solution resulted in a 4.5-fold photocurrent increase compared to pure water. When saturating the solutions with oxygen, the photocurrent was reduced by roughly 40%, which is attributed to O_2 acting as an electron scavenger. Upon introducing methanol in a gas flow even higher photocurrents were obtained (30% higher compared to liquid phase) and again a 4.5-fold increase was observed with regard to pure water vapor. When using air as the carrier gas (21% O_2) instead of inert N_2, the photocurrent only dropped by 8%, indicating the suitability of using a PEC cell for waste gas abatement. Preliminary experiments using ethanol and acetic acid also confirm its potential. Using infrared spectroscopy it was shown that more complete mineralization of methanol to CO_2 occurred in the presence of O_2, but also additional intermediates were formed and alternative reaction pathways involving methyl formate and dimethyl ether were proposed. This study highlights a tradeoff when using PEC cells for organic waste gas treatment: the presence of oxygen promotes more complete mineralization to CO_2, but limits the generated photocurrent and consequently H_2 evolution. Finally, the Faradaic efficiency toward H_2 evolution was determined to be 92% when using a methanol-rich gas flow as the PEC cell feed. We are hopeful this study has showcased the new application potential of energy-efficient (un-biased) PEC cells for waste gas after-treatment with the attractive advantage of simultaneous energy recovery and we look forward to discovering new advancements towards industrially relevant applications.

Experimental Section

Photo-electrochemical cell

The PEC cell design and membrane electrode assembly (MEA) are described and characterized in detail in earlier work.[12] In brief, the photo-anode (0.5 mg cm^{-2} P25 TiO_2 (Evonik) on Toray paper 030 (Fuel Cell Earth)) was calcined at 450°C for 2 h and embedded in 0.015 mg cm^{-2} Nafion® (Sigma Aldrich). Subsequently anode and cathode (0.09 mg cm^{-2} Pt@Carbon black (Umicore) on Toray paper 030) were fixed on opposite sides of a preconditioned Nafion® 117 membrane (Quintech) by hot-pressing between two teflon liners at 130°C for 2.5 min. The as-prepared MEA was mounted in the PEC cell by sandwiching the MEA between a graphite block (cathode side) and a transparent fused silica plate (anode side), both with grafted serpentine flow fields (Figure 4).

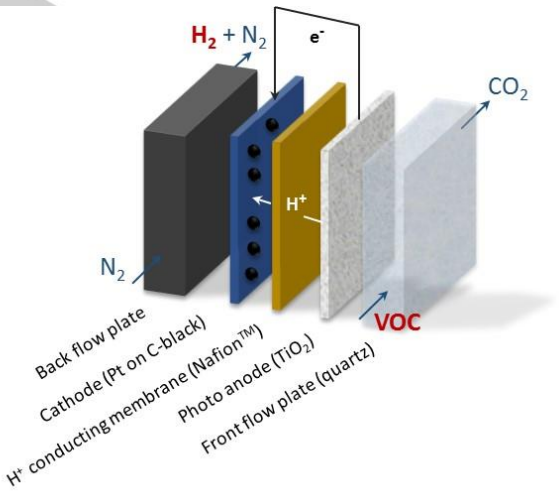

Figure 4. Schematic representation of the photo-electrochemical cell.

To irradiate the cell, a Philips Cleo 25 W UVA light source was positioned at a distance of 5 cm from the fused-silica plate, resulting in an incident intensity of 4 mW cm^{-2}, which roughly corresponds to the UV content of solar radiation on earth.

Aqueous phase experiments

Methanol (VWR Analytic, >99.8%) solutions were prepared in deionized water (<0.5 µS cm^{-1}) with concentrations of 0, 0.1, 1 and 5 wt%. In a first set of experiments each solution was purged with pure N_2 for 1 h in order to remove all traces of O_2. The purged solution was then pumped (Thermo Scientific FH10 peristaltic pump) through the anode compartment at a pumping

speed of 1.2 mL min^{-1}. After 1 h equilibration in dark conditions, a 90 s chrono-amperometric (CA) measurement was conducted under UV illumination using a potentiostat (Versastat 3, Princeton Applied Research). In order to study the effect of oxygen present in the system, the solutions were purged with synthetic air (21% O_2, Messer) for 1 h and analyzed likewise. The cathode compartment was flushed with N_2 at 50 mL min^{-1} at all times to avoid gas cap formation over the cathode.[25]

Gas phase experiments

Gas phase experiments were conducted in a fully automated gas test setup developed in our group.[14] In order to introduce methanol and/or water vapor in the gas flow, a gas wash bottle filled with either pure deionized water, or a 5 wt% aqueous methanol solution was mounted in the setup. Carrier gas was bubbled through this vessel at a steady flow rate of 50 mL min^{-1}. The carrier gas was pure N_2 or synthetic air containing 21% O_2 (Messer) to investigate the effect of oxygen on cell performance. According to Raoult's law for partial vapor pressures in ideal gas mixtures, a maximum theoretical methanol vapor concentration of 0.15 mol m^{-3} is thus attained. The composition of the gas stream was continuously analyzed on-line by Fourier Transform Infrared Spectroscopy (FTIR, Thermo Fisher Scientific Nicolet 380 with ZnSe windows and 2 m heated gas cell). A humidity sensor (Vaisala) was attached to the gas outlet. The cathode compartment was flushed with N_2 at 50 mL min^{-1} at all times to avoid gas cap formation over the cathode.[25] After equilibration of the outlet concentrations, long chrono-amperometric measurements (20 min) were conducted using the potentiostat, while simultaneously monitoring the changes in outlet gas composition by FTIR.

H_2 evolution efficiency

The Faradaic efficiency for H_2 evolution was determined using a quantitative gas analyzer (Hiden Analytical). An inert argon flow was bubbled at a rate of 25 mL min^{-1} through a 5 wt% aqueous methanol solution in MilliQ water, sent through the anode compartment and then to the detection unit. The cathode compartment was flushed with pure N_2 at 25 mL min^{-1} at all times. The gas evolution was corrected for slight fluctuations in flow rate by means of the N_2 signal. To ensure a measurable quantity of H_2 well above the detection limit of the apparatus, the cell was irradiated by a 400 W broad spectrum Xe source (200-750 nm, Oriel 66984, Newport) adjusted so the incident intensity was 100 mW cm^{-2}. The generated photocurrent was collected by the potentiostat. Ultimately, the Faradaic efficiency was determined as the ratio of the actual amount of H_2 collected, over the theoretical amount of H_2 that can be produced from the generated photocurrent, as calculated by the formula (Eq. 17):

$$\text{Theoretical } H_2 \text{ (mL)} = (Q\ v)/(n\ F) \qquad \text{(Eq. 17)}$$

with Q the total amount of photogenerated charge (C), v the molar gas volume (22400 mL mol^{-1}), n the number of electrons in the reaction (2) and F the Faraday constant (96485.3 C mol^{-1}).

Acknowledgements

S.W.V. and J.R. acknowledge the Research Foundation – Flanders (FWO) for a post-doctoral fellowship. T.B. and J.A.M. acknowledge the Flemish government for long-term structural funding (Methusalem). Ir. Nicolaas Schewyck is greatly thanked for his experimental work during his master thesis.

Keywords: Photo-electrochemical (PEC) cell • methanol • Titanium dioxide (TiO2) • gas phase • hydrogen

[1] A. Kudo, Y. Miseki, *Chem. Soc. Rev.* **2009**, *38*, 253–278.
[2] K. Maeda, K. Teramura, D. Lu, T. Takata, N. Saito, Y. Inoue, K. Domen, *Nature* **2006**, *440*, 295–295.
[3] S. W. Verbruggen, *J. Photochem. Photobiol. C Photochem. Rev.* **2015**, *24*, 64–82.
[4] P. Lianos, *J. Hazard. Mater.* **2011**, *185*, 575–90.
[5] B. Seger, P. V Kamat, *J. Phys. Chem. C* **2009**, *113*, 18946–18952.
[6] J. Rongé, S. Deng, S. Pulinthanathu Sree, T. Bosserez, S. W. Verbruggen, N. Kumar Singh, J. Dendooven, M. B. J. Roeffaers, F. Taulelle, M. De Volder, et al., *RSC Adv.* **2014**, *4*, 29286–29290.
[7] J. Georgieva, *J. Solid State Electrochem.* **2011**, *16*, 1111–1119.
[8] J. Georgieva, S. Armyanov, I. Poulios, A. D. Jannakoudakis, S. Sotiropoulos, *Electrochem. Solid-State Lett.* **2010**, *13*, P11.
[9] J. Georgieva, S. Armyanov, I. Poulios, S. Sotiropoulos, *Electrochem. commun.* **2009**, *11*, 1643–1646.
[10] R. Li, Y. Weng, X. Zhou, X. Wang, Y. Mi, R. Chong, H. Han, C. Li, *Energy Environ. Sci.* **2015**, *8*, 2377–2382.
[11] K. O. Iwu, A. Galeckas, A. Y. Kuznetsov, T. Norby, *Electrochim. Acta* **2013**, *97*, 320–325.
[12] J. Rongé, D. Nijs, S. Kerkhofs, K. Masschaele, J. A. Martens, *Phys. Chem. Chem. Phys.* **2013**, *15*, 9315–25.
[13] J. Chen, B. Li, J. Zheng, S. Jia, J. Zhao, H. Jing, Z. Zhu, *J. Phys. Chem. C* **2011**, *115*, 7104–7113.
[14] T. Tytgat, B. Hauchecorne, M. Smits, S. W. Verbruggen, S. Lenaerts, *J. Lab. Autom.* **2012**, *17*, 134–143.
[15] S. W. Verbruggen, K. Masschaele, E. Moortgat, T. E. Korany, B. Hauchecorne, J. A. Martens, S. Lenaerts, *Catal. Sci. Technol.* **2012**, *2*, 2311–2318.
[16] M. Dumortier, T. Bosserez, J. Rongé, J. A. Martens, S. Haussener, *J. Phys. Chem. C* **2016**, *120*, 3705–3714.
[17] S. W. Verbruggen, M. Keulemans, M. Filippousi, D. Flahaut, G. Van Tendeloo, S. Lacombe, J. A. Martens, S. Lenaerts, *Appl. Catal. B Environ.* **2014**, *156–157*, 116–121.
[18] S. W. Verbruggen, M. Keulemans, B. Goris, N. Blommaerts, S. Bals, J. A. Martens, S. Lenaerts, *Appl. Catal. B Environ.* **2016**, *188*, 147–153.
[19] G. L. Chiarello, M. H. Aguirre, E. Selli, *J. Catal.* **2010**, *273*, 182–190.
[20] M. El-Roz, P. Bazin, F. Thibault-Starzyk, *Catal. Today* **2013**, *205*, 111–119.
[21] R. T. Carr, M. Neurock, E. Iglesia, *J. Catal.* **2011**, *278*, 78–93.
[22] R. Wang, K. Hashimoto, A. Fujishima, M. Chikuni, E. Kojima, A. Kitamura, M. Shimohigoshi, T. Watanabe, *Nature* **1997**, *388*, 431–432.

[23] N. Stevens, C. I. Priest, A. R. Sedev, J. Ralston, *Langmuir* **2003**, *19*, 3272–3275.

[24] X. Feng, J. Zhai, L. Jiang, *Angew. Chemie Int. Ed.* **2005**, *44*, 5115–5118.

[25] C. Ampelli, G. Centi, R. Passalacqua, S. Perathoner, *Energy Environ. Sci.* **2010**, *3*, 292.

Entry for the Table of Contents (Please choose one layout)

Layout 1:

FULL PAPER

An all-gas-phase un-biased photo-electrochemical cell converts organic pollutants in air while recovering energy as hydrogen gas

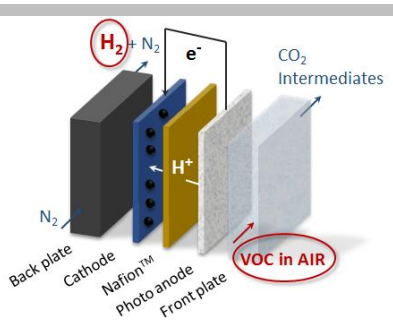

Sammy W. Verbruggen, Myrthe Van Hal, Tom Bosserez, Jan Rongé, Birger Hauchecorne, Johan A. Martens, Silvia Lenaerts*

Page No. – Page No.

Harvesting hydrogen gas from air pollutants with an un-biased gas phase photo-electrochemical cell